



Power Quality Improvement in a PSO MPPT Based Solar PV Plant Integrated Utility Grid by Employing a Novel Adaptive Current Regulator using ANFIS Controller

Mr. S. Jagadish Kumar Assistant Professor, Department of Electrical and Electronics Engineering,
JNTUH College of Engineering, Jagtial, Telangana-505501, India.

Email : jagadishkumar1@gmail.com

Nampally Bhanuchander M.Tech Student, Department of Electrical and Electronics Engineering,
JNTUH College of Engineering, Jagtial, Telangana-505501, India.

Email: bhanupawan7795@gmail.com

Abstract—Harmonics are created during the integration of solar PV plants and due to non linear loads into distribution systems a novel adaptive current regulator is employed for the grid interfacing voltage source inverter. In addition, a high-gain dc–dc converter with a PSO MPPT algorithm is designed to achieve the high voltage level at the common dc bus. To determine three-phase reference currents the proposed adaptive current regulator is designed by using a ADVANSED NEURO FUZZY INTERFACE SYSTEM. They are used to generate the three-phase compensating currents for suppressing the harmonics present in the system. The proposed method has several merits, such as better harmonic mitigation ability, adaptive behaviour, improved stability, and lesser settling time .The system performance with the proposed current control regulator is analyzed via MATLAB/Simulink.

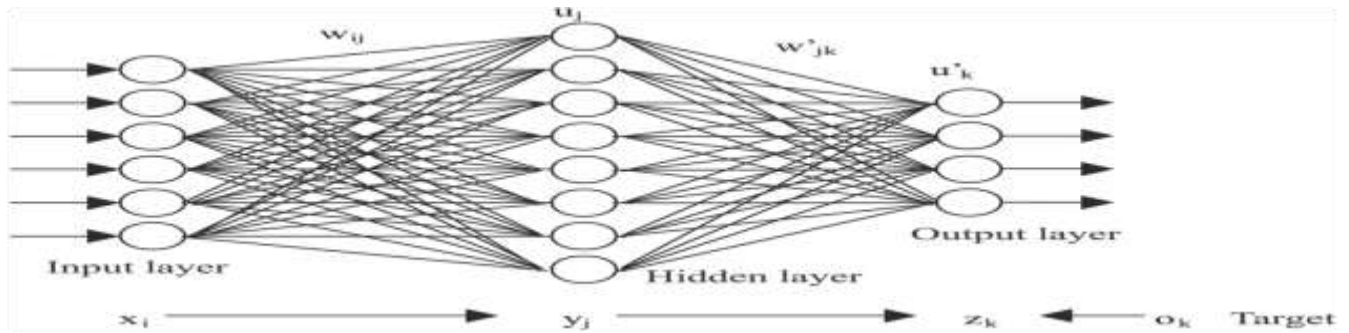
I.INTRODUCTION

RENEWABLE power injection to existing utility grid is becoming essential to meet the electricity demand in the future to come. The massive penetration of renewable energy sources (RES) can reduce the use of fossil-fuel as well as protect the environment from greenhouse gas emission. It has few limitations like low generating voltages, difficult in tracking maximum power point (MPP) due to sporadic nature of solar irradiance, and poor power quality due to the presence of power electronic converters and varying connected loads in the system

DC–DC boost converters are utilized to match low voltages of the PV system at the common dc-link bus terminals. The drawbacks with the conventional dc–dc converters are sudden rise in input current, high power loss during switching, and maximum diode reverse current Hence, dc microgrid associated with the conventional converters suffers from more losses, high strain, and less efficiency I

Recurrent neural network (RNN) has been employed to reduce the harmonics produced in the system, and also to get superior control over grid injected reactive power. RNN is an effective control technique compared with the conventional control schemes because of its self-adjustment capability during system parameter variations, and it works well under the noisy conditions and better performance during large load change [. The performance of the proposed RNN current controller mainly depends on the use of efficient training algorithm. In this article, a novel adaptive [Hebbian least mean square (LMS) based RNN]

III. Control of Voltage Source Inverter by RECURRENT NEURAL NETWORK



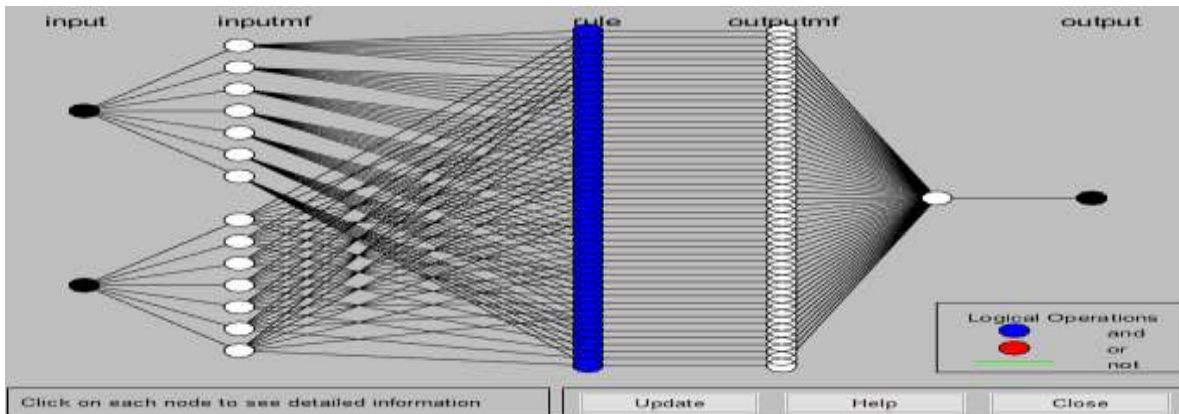
RNN-current control structure trained by the Hebbian LMS algorithm helps in achieving system stability quickly and consequently following better power quality. Therefore, it is best suited for the closed-loop control applications. Thus, the deployment of proposed RNN inner current-loop control function maintains improved quality of currents to the utility grid. The active and reactive powers are regulated by d- and q-axis control loops.

ADVANCED NEUROFUZZY INTERFACE SYSTEM CONTROLLER:

CONSTRAINTS OF ANFIS:

ANFIS is much more complex than the fuzzy inference systems and is not available for all of the fuzzy inference system options. Specifically, ANFIS only supports Sugeno-type systems, and these must have the following properties:

- Be first or zero order Sugeno -type systems.
- Have a single output, obtained using weighted average defuzzification. All output membership functions must be the same type and either linear or constant.
- Have no rule sharing. Different rules cannot share the same output membership function namely the number of output membership functions must be equal to the number of rules.



IV. Simulation results

Testing and validation process of the developed ANFIS:

Once the model structure and parameters have been identified, it is necessary to validate the quality of the resulting model. In principle, the model substantiation should not only validate the accuracy of the model, but also verify whether the model can be easily interpreted to give a better understanding of the modelled process. It is therefore important to combine data-driven validation, aiming at checking the accuracy and

robustness of the model, with more subjective validation, concerning the interpretability of the model. There will usually be a challenge between flexibility and interpretability, the outcome of which will depend on their relative importance for a given application. While, it is evident that numerous cross validation methods exist, the choice of the suitable cross-validation method to be employed in the ANFIS is based on a trade- off between maximizing method accuracy and stability

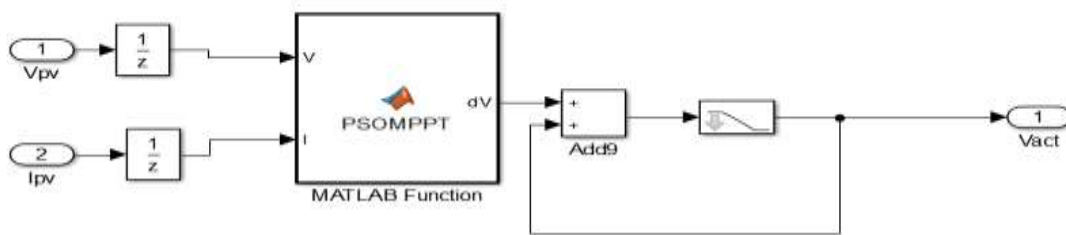


FIG5: Simulink model of PSO MPPT

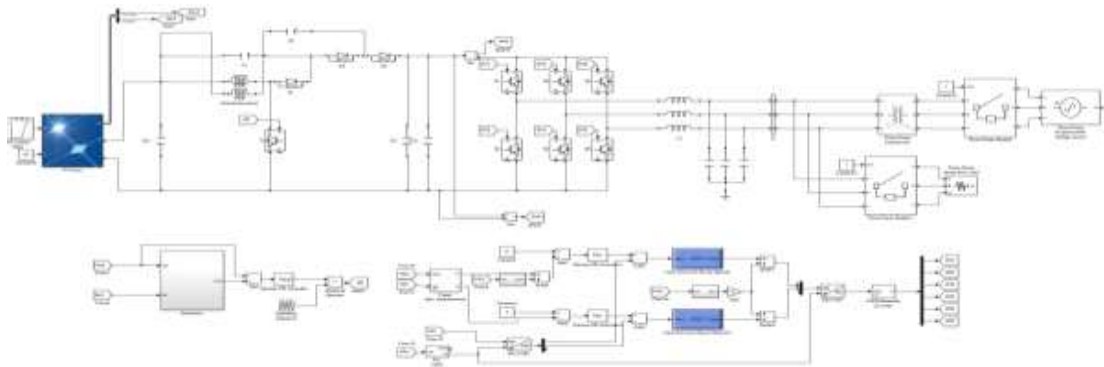


FIG6: Simulink model of proposed system

To assure the controller performance under different system conditions, it is analyzed under five different cases such as by changing solar irradiance, transient linear load, transient nonlinear load, L–G fault on grid side, and unbalanced grid voltage. These test cases are described as follows.

Test Case 1: In this study, Solar irradiance is changed with a step change from 1000 to 600 W/m² at $t = 0.2$ s and again it increased linearly in the duration of 0.6–0.8 s.

In this case, the outer voltage loop is fuzzy voltage regulator, and the inner current loops are fuzzy and RNN controllers. Fig. 8(a), (c), and (e) shows the performance characteristics of the proposed system with conventional fuzzy current controller, whereas Fig. 8(b), (d), and (f) shows the performance characteristics of the proposed system by employing ANFIS controller. Fig. 8(a) and (b) shows the PV terminal voltage and current at the input of boost converter, and change in PV current corresponds to the irradiance change, respectively

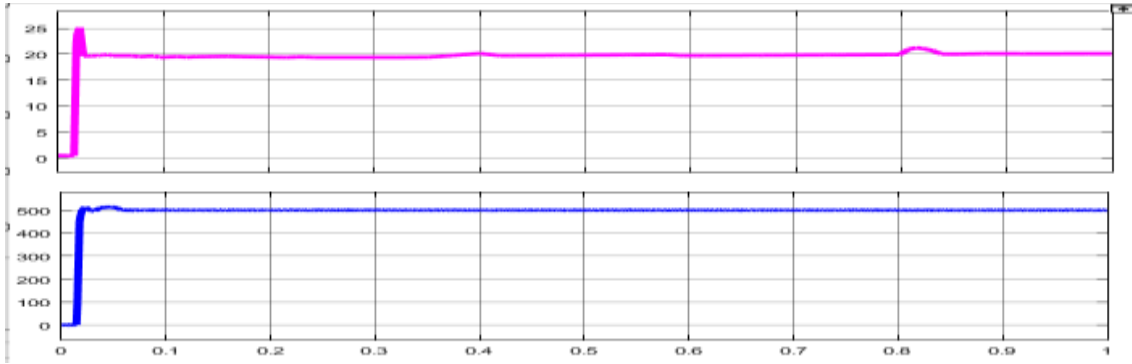
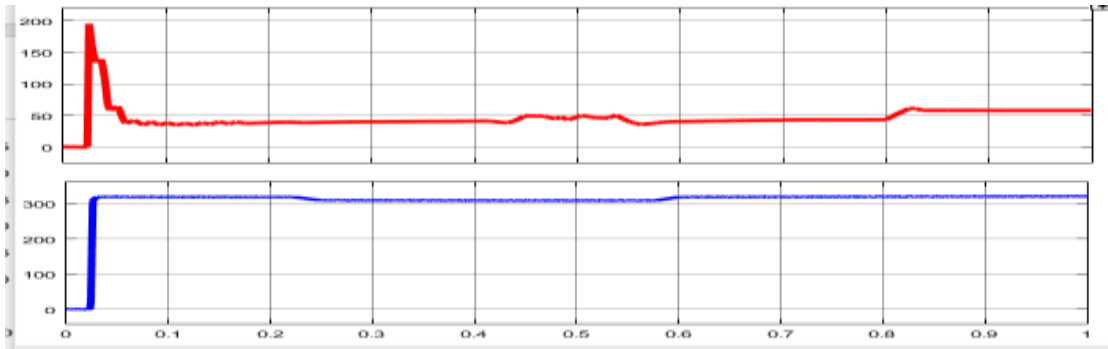
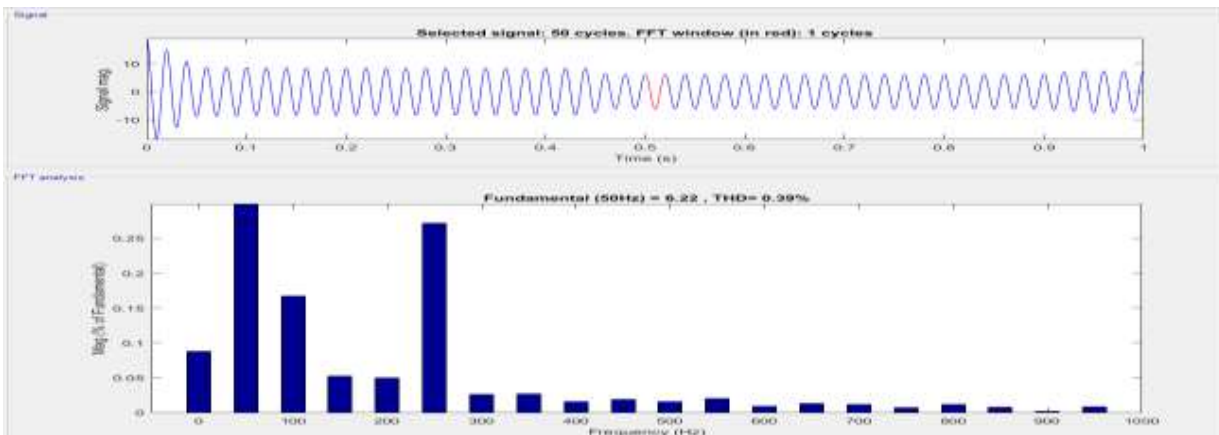
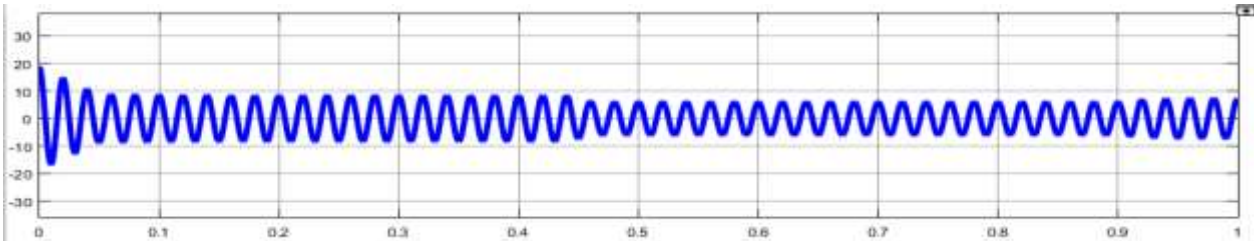


Fig. 8. Performance parameters. Case 1: (a) and (b) Point of common coupling (PCC) terminal current and voltage.



(c) and (d) Current and voltage at common dc bus.



(e) grid current thd%=0.39

Test Case 2: In this case, by checking the dynamic performance is investigated by increasing the linear load in the system,

which is observed in Fig. 9 during $t = 0.4-0.8$ s. Fig. 9(a) and (b) shows the three-phase currents and voltages under the load change, respectively. The change in the load reflects on the grid currents. Fig. 9(c) and (d) depicts the current and voltage characteristics of the conventional fuzzy controller and the proposed RNN current controller, respectively. By observing Fig. 9(c) and (d), the proposed ANFIS controller shows better stability performance over the conventional fuzzy logic controller by maintaining the constant voltage. Similarly, Fig. 9(e) and (f), shows %THD content for the grid current during dynamic load change with fuzzy and proposed ANFIS controller is 0.36%. In this condition, THD content of the proposed controller has been found very less compared to the conventional controller

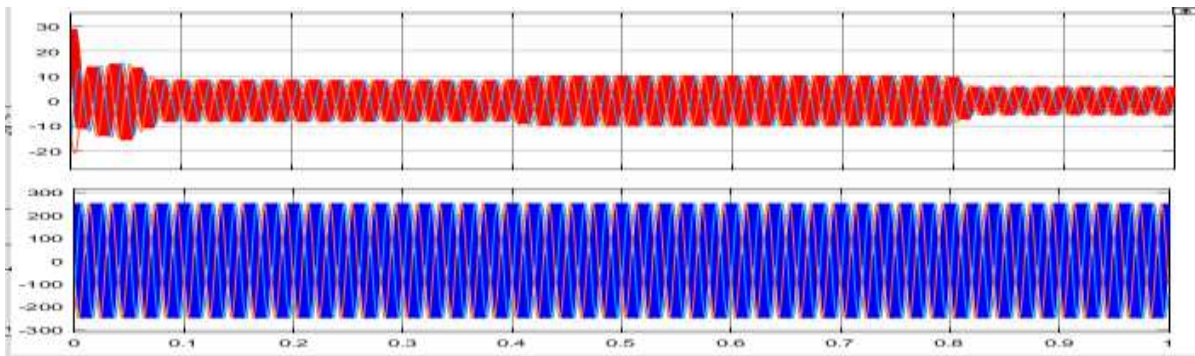
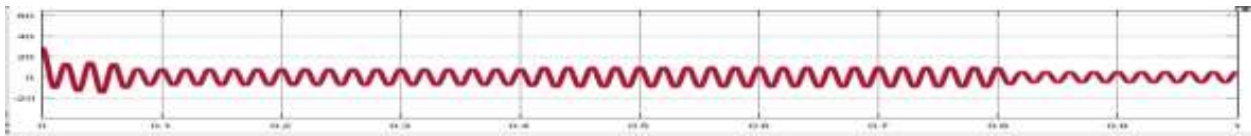
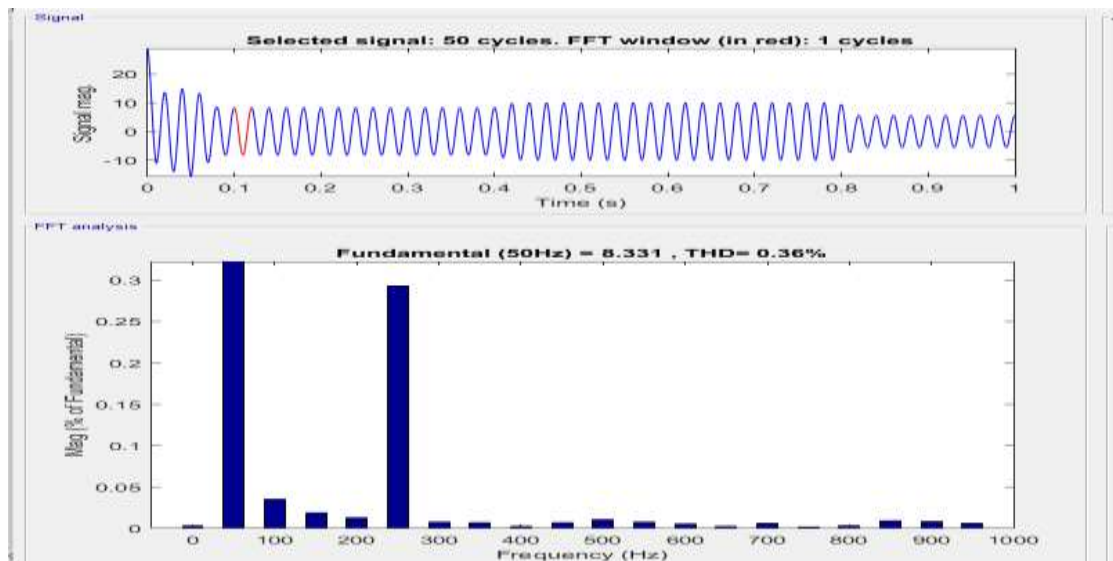


Fig. 9. Performance parameters. Case 2: (a) and (b) PCC terminal current and voltage.

(c) and (d) Current and voltage at common dc bus.



e.grid side current



(f) %THD of grid-side current=0.36%

Test Case 3: In this case, the system dynamic performance is investigated by adding the nonlinear load to the system,

which is shown in Fig. 10 during $t = 0.3\text{--}0.8$ s. Fig. 10(a) and (b) shows the three-phase grid currents, and voltages under nonlinear load change, respectively. It is evident from the figure that the change in the nonlinear load reflects on the grid currents. Fig. 10(c) and (d) depicts the current and voltage characteristics of the conventional PI controller and proposed ANFIS controller, respectively. By observing Fig. 10(c) and (d), the proposed ANFIS controller shows better stability and settling performance over the conventional fuzzy logic controller. Similarly, Fig. 10(e) and (f) shows %THD content for the grid current during transient nonlinear load change with fuzzy logic and proposed ANFIS controller is 1.03% respectively. In this condition, THD content of the proposed controller has been found satisfactorily compared with the conventional controller.

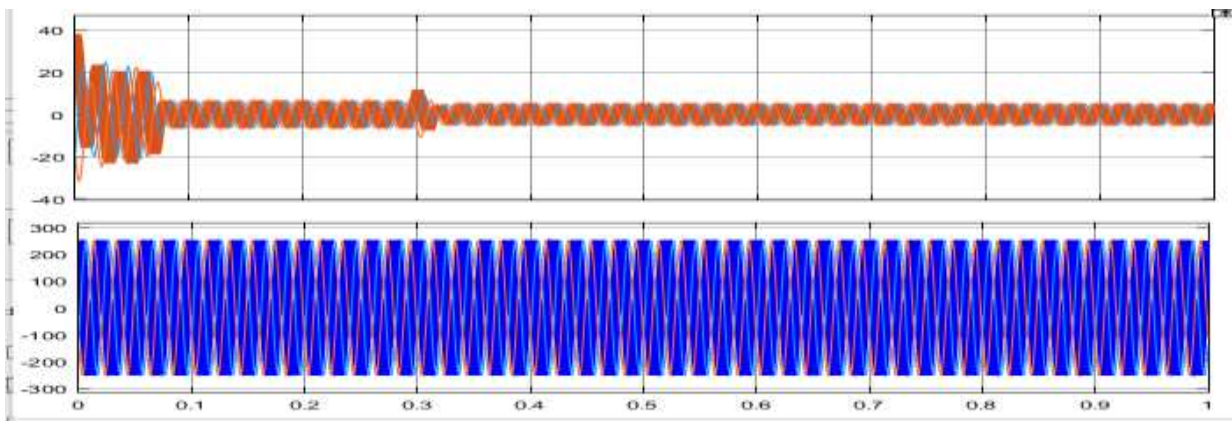
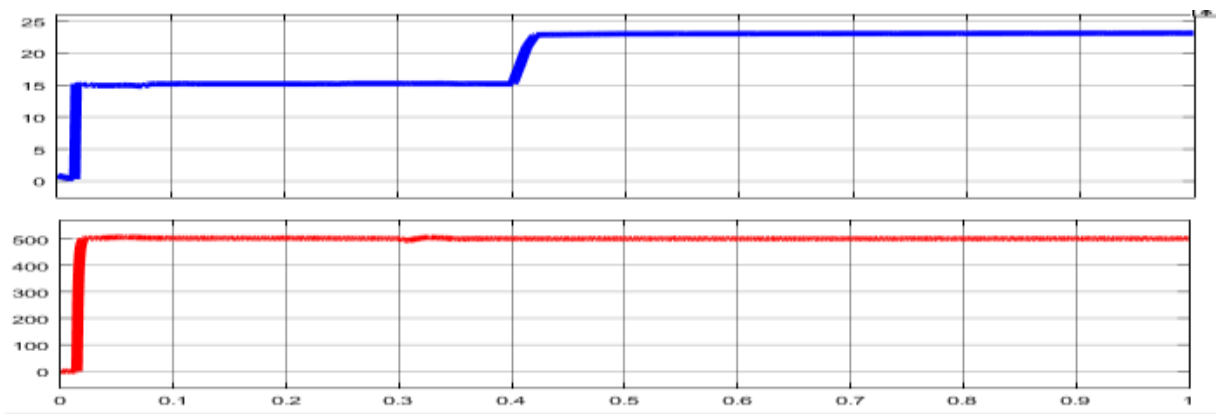
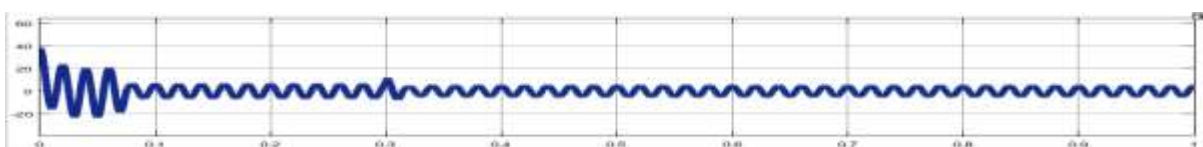


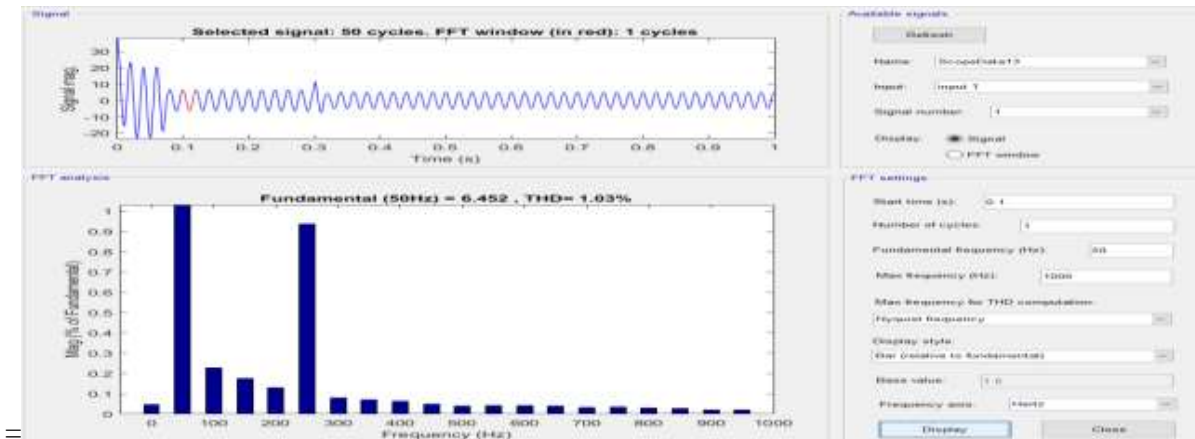
Fig. 10. Performance parameters. Case 3: (a) and (b) Grid-side current and voltage



(c) and (d) Current and voltage at common dc bus



(e) grid side current



Test Case 4: In this study, an L–G fault is created at grid side during $t = 0.3–0.8$ s.

Fig. 11(a) and (b) depicts the three-phase currents and voltages under system fault condition. In this condition, the grid current is raising high because of an L–G fault is created in grid side. Fig. 11(c) and (d) depicts the current and voltage characteristics of the conventional fuzzy controller and proposed RNN current controller correspondingly. By observing Fig. 11(c) and (d), the proposed ANFIS controller shows better performance . Similarly, Fig. 11(e) and (f) shows %THD content for the grid current during an L–G fault condition with proposed ANFIS controller is 0.34 % respectively. In this condition, harmonic content of the proposed controller has been found very less compared with the conventional controller.

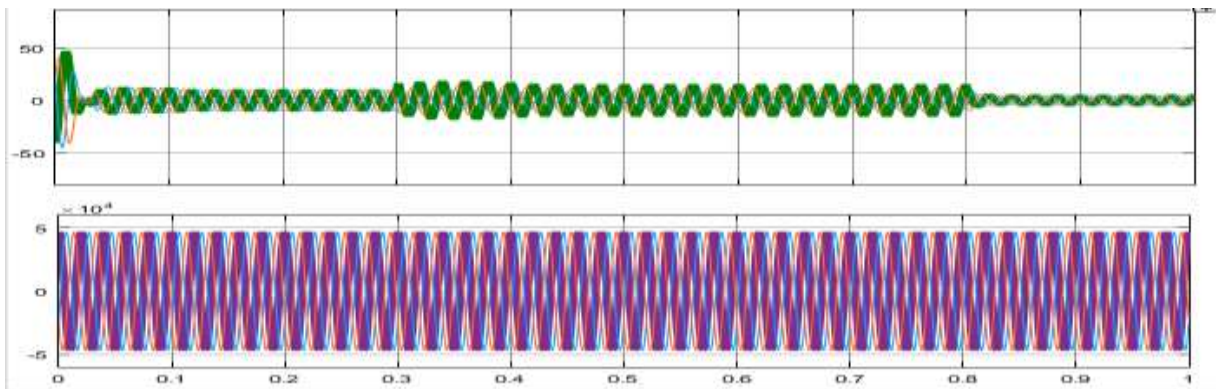
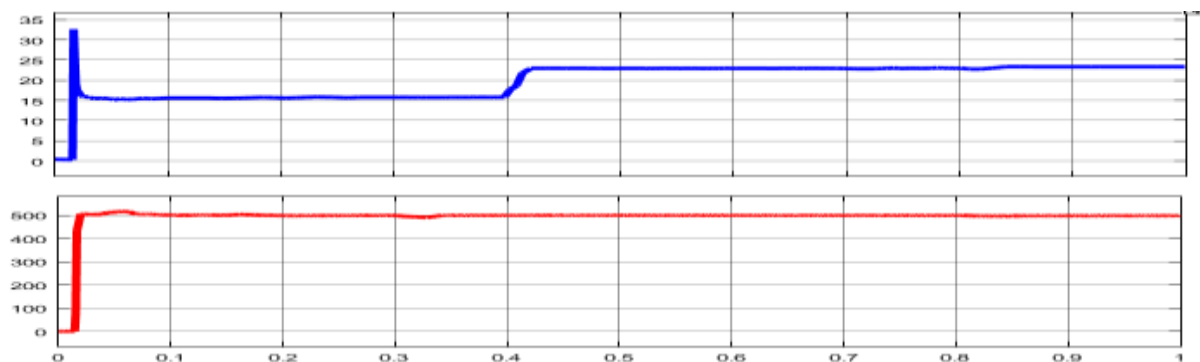
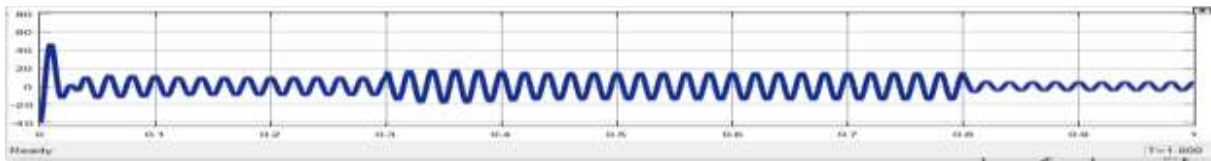


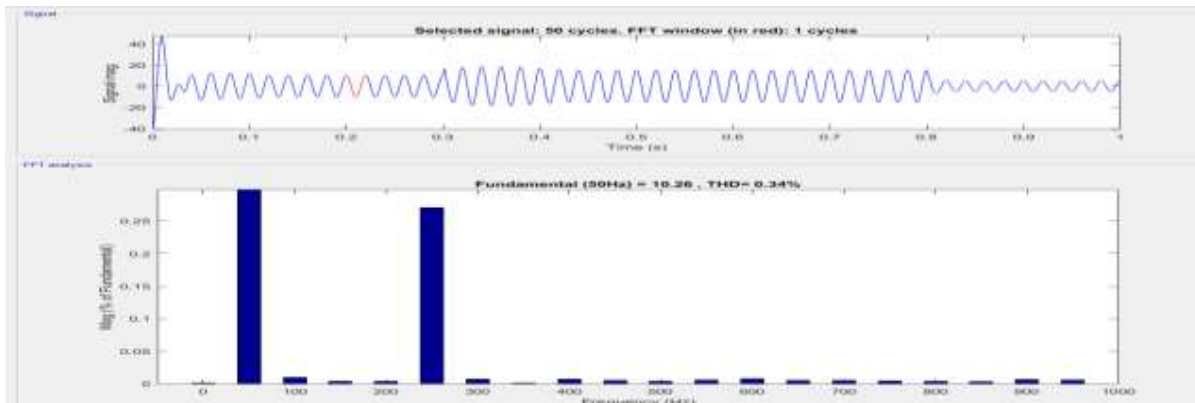
Fig. 11. Performance parameters. Case 4: (a) and (b) Grid-side current and voltage



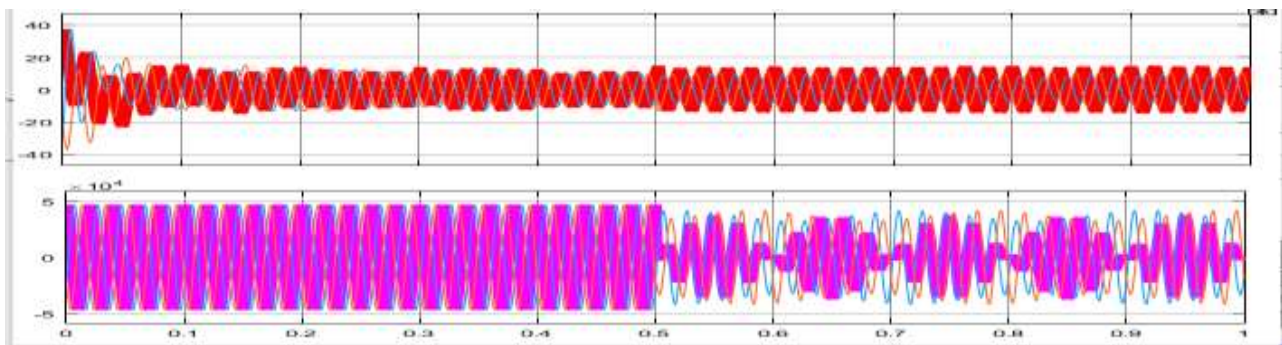
. (c) and (d) Current and voltage at common dc bus.



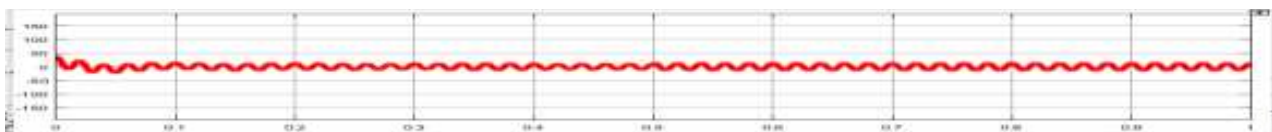
(e) grid current



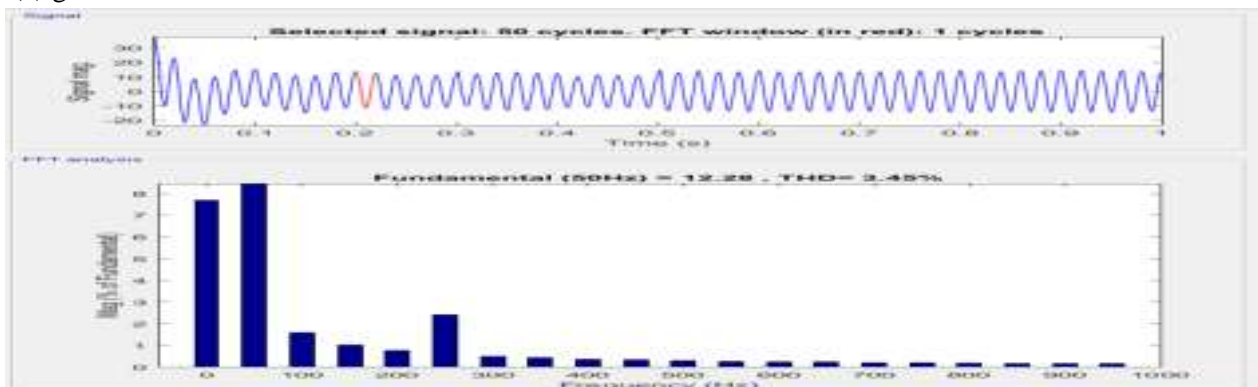
(f) %THD of grid-side current=0.34%



(c) and (d) Current and voltage at common dc bus.



(e) grid current



(f) %THD of grid-side current.=3.45%



Comparison table for test cases of THD

	Kalman mppt with pi controller THD %	PSO mppt with ANFIS controller THD %
Test case 1(change in irradiance)	1.68%	0.39%
Test case2(dynamic linear load)	1.72%	0.36%
Test case3(dynamic non linear load)	3.75%	1.03%
Test case4(L-G fault)	1.57%	0.34%
Test case5(unbalanced grid voltage)	11.45%	3.45%

VIII.CONCLUSION

In the current context, power generation from renewable sources, particularly solar, is evolving. PV plant integration to the utility grid is hampered by a number of drawbacks, including low PV terminal voltage and poor power quality during dynamic demand variations. To address these disadvantages, our study focuses primarily on the performance of employing a high-gain boost converter with PSO MPPT to achieve a high voltage level. Furthermore, an ANFIS control approach learned with to obtain improved power quality, i.e., percent THD is well under the limit under different operating circumstances. A new improved PSO MPPT algorithm is developed to overcome the disadvantages of Kalman mppt algorithm by introducing opposition based learning and worst population elimination methods. The proposed algorithm tracks the global MPP with very less tracking time using the best initial population and also reduces larger exploration of search space. The proposed algorithm improves the overall system performance and it is superior to conventional algorithm in terms of tracking speed, THD value of grid current for different test cases is reduced .

REFERENCES

- [1] S. Manaffam, M. Talebi, A. K. Jain, and A. Behal, "Intelligent pinning based cooperative secondary control of distributed generators for microgrid in islanding operation mode," IEEE Trans. Power Syst., vol. 33, no. 2, pp. 1364–1373, Mar. 2018.
- [2] S. Mishra and P. K. Ray, "Power quality improvement using photovoltaic fed DSTATCOM based on JAYA optimization," IEEE Trans. Sustain. Energy, vol. 7, no. 4, pp. 1672–1680, Oct. 2016.
- [3] R. Langella, A. Testa, J. Meyer, F. Moller, R. Stiegler, and S. Z. Djokic, "Experimental-based evaluation of PV inverter harmonic and interharmonic distortion due to different operating conditions," IEEE Trans. Instrum. Meas., vol. 65, no. 10, pp. 2221–2233, Oct. 2016. .